# Segregation and Fluidization Behavior of Poly-disperse Mixtures of Biomass and Inert Particles

Paola Brachi[a], Riccardo Chirone[a], Francesco Miccio [b], Michele Miccio[c] ,Giovanna Ruoppolo[a]

[a]Institute for Research on Combustion, (IRC-CNR), P.le Tecchio 80, 80125 Napoli, Italy
[b]Institute of Science and Technology for Ceramics (ISTEC-CNR), via Granarolo 64, 48018 Faenza (RA), Italy
[c]Department of Industrial Engineering, University of Salerno, via Giovanni Paolo II 132, 84084 Fisciano (SA), Italy
p.brachi@cnr.irc.it

This paper reports on the results of an experimental study aimed at investigating the fluidization and segregation behavior of poly-disperse binary mixtures consisting of small and dense inert particles mixed with less dense and coarse pieces of biomass fuels. In more details, orange peels (OP), conditioned to a moisture content of about 6% wt. and cut in square pieces (0.5 cm x 0.5 cm), were used as biomass feedstock. Three different materials (i.e., Ticino sand, quartz sand, alumina powder and alumina spheres) were tested as inert bed component in order to determine the prevalence of the effect of either size or density on the fluidization and segregation behavior of the investigated binary systems. Fluidization experiments were performed at room temperature in order to prevent that the formation of endogenous bubbles from devolatilizing fuel particles could come into play, which also impacts mixing and segregation phenomena in real fluidized bed reactors. Tests with different biomass weight fraction in the bed ($X_B$) were performed both to study the effect of the bed composition on the characteristic velocities of the investigated binary systems (i.e., minimum and complete fluidization velocities) and to determine their maximum batch loading, i.e. the critical value of $X_B$ beyond which the fluidization quality deteriorate (e.g., channelling, irreversible segregation, slugging).

## 1. Introduction

Several unique operational advantages, like feedstock flexibility, uniform temperature, intense solids mixing and efficient heat transfer, have made fluidized bed reactors the most efficient and widely used technological option in energy production/conversion processes (Ruoppolo et al., 2013). Most of the applications of fluidized beds involve biomass particles co-fluidized with much denser and more regular inert particles, which are typically used to ensure proper fluidization (e.g., preventing bridging and channeling) and to provide additional heat capacity in the bed (Brachi et al., 2016). However, the presence of particles differing in one or more of their constitutive properties (i.e., shape, size, density etc.) could give rise to some drawbacks in fluidized beds. One of the most undesirable is the tendency of the particles to be segregated along the bed as it causes unstable fluidization patterns and reduces the heat and mass exchange rates. Therefore, a major concern for processes involving the fluidization of dissimilar components relies on setting the operating conditions (e.g., particle sizes, biomass weight fraction, type of inert bed material, etc.) in a way that the advantages associated with the mixing of the solids can be maximized. In spite of all the research findings reported in the literature, there has been little work of both comprehensive and fundamental nature, which could delineate more general principles or provide rules helpful in resolving multiphase flow drawbacks for beds involving biomass particles (Cui and Grace, 2007). Fundamental work on particulate processes has mostly been focused on dry spherical particles of narrow size distributions  shapes (Formisani et al., 2008), with limited extension to others with irregular shape. Therefore, further research is required in order to provide a general understanding of the interactions among particles in a heterogeneous mixture. In an attempt to tackle this knowledge gap, an experimental study aimed at understanding segregation and fluidization characteristics of poly-disperse binary mixtures of biomass and inert particles was carried out and the results are presented in this work. Orange peels, i.e., the solid byproduct of orange juice processing, were selected as the biomass

component due to the increasingly interest they are gaining as a potential feedstock for bioenergy and biofuels production (Volpe et. al, 2015). Several granular solids having the same density but different size or with the same size but different density were tested as inert bed material in order to determine the prevalence of the effect of either size or density on the fluidization and segregation behavior of binary systems. In particular, fluidization experiments at room temperature were conceived to prevent the formation of (endogenous) volatile matter bubbles around devolatilizing fuel particles (Bruni et al., 2002), which also impact mixing and segregation phenomena in real fluidized bed reactors.

## 2. Experimental

### 2.1 Inert bed materials and biomass feedstock preparation and characterization

Peels of fresh oranges were used in this work as biomass feedstock. The peels were separated from the pulp by hand and afterwards subjected to preliminary operations of drying and size-reduction. In more details, raw orange peels (74.7 % wt. moisture content) were conditioned down to a moisture content of about 6% wt., which represents the equilibrium value that the raw peels reached when left in a laboratory fume hood at room temperature for 2 days. After drying, peels were cut into slabs (0.5 cm × 0.5 cm) having a thickness of few millimeters and then stored in a desiccator to minimize the moisture uptake. Four types of granular solids were tested in this work as bed material to assist the biomass fluidization, namely: 1. fine quartz sand in the size range of 100-250 µm (FS); 2. coarse Ticino sand in the size range of 150-400 µm (CS); 3. fine commercial γ-alumina powder (PURALOX SCCA-150/200, SASOL) in the size range of 50-250 µm (FA): and 4. coarse commercial γ-alumina spheres (PURALOX alumina spheres 0.3/180, SASOL) in the size range of 200-400 µm (CA). Images of the bed components used in the experiments are shown in Figure 1.
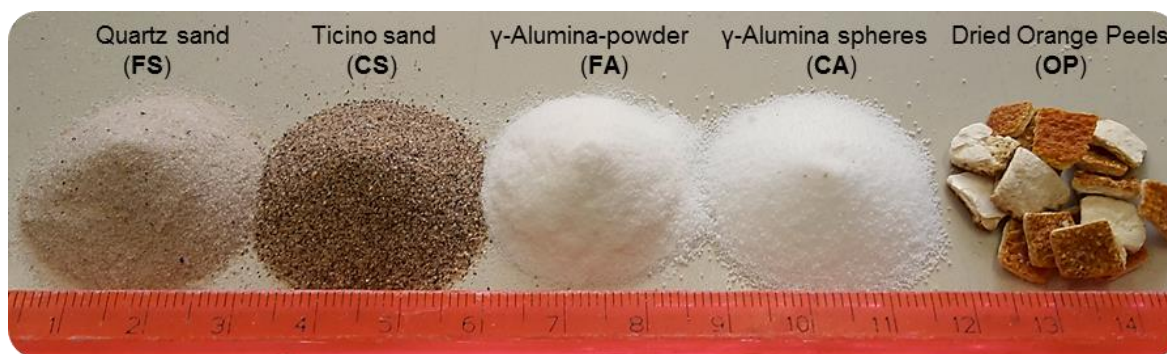


*Figure 1: Pictures of inert materials and biomass feedstock.*

The particle-size distribution of the inert materials was determined by using a laser diffraction analyzer (Mastersizer 2000, Malvern Instrument Inc.), with an analytical size range of 0.2–2000 µm. Granular solids were characterized by the Sauter mean diameter D[3,2], which is particularly suitable for describing mean size of a given particle distribution in the context of interphase processes in which the specific surface area plays a major role (drag forces or heat exchange). Five replicate measurements were performed for each sample and the D[3,2]-values shown in Table 1 are the mean value of the data provided by the Malvern Mastersizer 2000 software. A Quantachrome Ultrapycnometer 1000 helium gas pycnometer was used for the determination of the skeletal density ($\rho_S$) of both orange peels and inert solids. Measurements were performed after the samples were oven dried at 105 ± 5 °C for 24 h. The $\rho_S$-values shown in Table 1 represent the average of five measured values. Nitrogen adsorption/desorption experiments at -196 °C were performed by using a Quantachrome Autosorb 1-C instrument in order to determine the total pore volume (PV, cc/g) of both orange peels and inert bed materials. Before the adsorption measurements, samples of the inert materials were outgassed overnight at 150 °C whereas orange peels were outgassed at 120 °C in order to prevent any devolatilization processes. The $\rho_S$ and PV data were used for the estimation of the envelope particle density ($\rho_P$) of samples by means of the following Eq(1):

$$\rho_P = \frac{\rho_S}{1+PV \cdot \rho_S} \tag{1}$$

where $\rho_S$ and PV are given g/cc and cc/g, respectively. Loose ($\rho_{lb}$) and packed ($\rho_{tb}$) bulk densities of bed components were determined from the sample weight and volume, using standard techniques. In particular, the bulk density was calculated as the ratio of the mass to the volume (including the contribution of the interparticle void volume) of an untapped sample, poured into a graduated cylinder without compacting. Conversely, the tapped density was obtained by mechanically tapping a graduated cylinder containing the

sample until no further volume change was observed. Graduated cylinders of different sizes (i.e., 100-ml and 500-ml) were used in this work to take account of the wall effect on the arrangement of the sample particles. Three measurements were performed for each cylinder, and bulk densities shown in Table 1 represent the average of the six measured values. Based on the obtained mean particle size and the density data, inert bed materials and OP slabs were classified according to Geldart's classification scheme, which is valid only for air-fluidized bed at ambient conditions (see Table 1).

*Table 1: Properties of biomass and inert particles used in this study*

|  | Quarz Sand FS | Silica Sand CS | $Al_2O_3$ powder FA | $Al_2O_3$ spheres CA | Orange peels OP |
|---|---|---|---|---|---|
| Souter diameter, D[3,2] (µm) | 139.8 | 209.9 | 123.7 | 255.3 | n.a. |
| Skeletal density, $\rho_s$ (kg/m$^3$) | 2813.5 | 2650.6 | 3986.9 | 3986.9 | 671.7 |
| Particle density, $\rho_p$ (kg/m$^3$) | 2813.5 | 2650.6 | 1250.3 | 1479.7 | 667.7 |
| Loose-bulk density, $\rho_{lb}$ (kg/m$^3$) | 1444.6 | 1367.1 | 761.1 | 823.2 | 230.2 |
| Packed-bulk density, $\rho_{pb}$ (kg/m$^3$) | 1575.0 | 1537.1 | 824.1 | 870.1 | 273.9 |
| Total pore volume, PV (cc/g) | 0 | 0 | 0.549 | 0.425 | $8.86 \cdot 10^{-3}$ |
| Group of Geldart's classification | B | B | A | B | D |

## 2.2 Experimental apparatus and test procedures

Fluidization tests at room temperature were performed in a cylindrical column (100 mm inner diameter and 750 mm height) made of transparent glass in order to facilitate visual observation of the fluidization pattern and movement of particles in the bed during the experiments. A 6-mm-thick sintered-glass gas distributor disk (nominal pore size of 16 – 40 µm) located at the bottom of the column supported the bed materials and ensured a uniform distribution of the fluidizing air. The pressure acquisition system was composed of two piezoresistive pressure sensors (GE Druck PTX 7200 Series) connected to a USB data acquisition device (PICO TC-08 Data Logger and TC-08 Terminal Board ) and located the first one just a few centimeters above the distributor plate, the second one in the freeboard. Further details of the experimental apparatus are provided elsewhere (Brachi, 2016). Fluidization experiments were performed on beds containing either only inert particles or binary mixtures obtained by mixing predetermined amounts of orange peels and granular solids while holding the bed aspect ratio nearly constant (i.e., H/D ≈ 2.2 ± 0.2), as shown in Table 2.
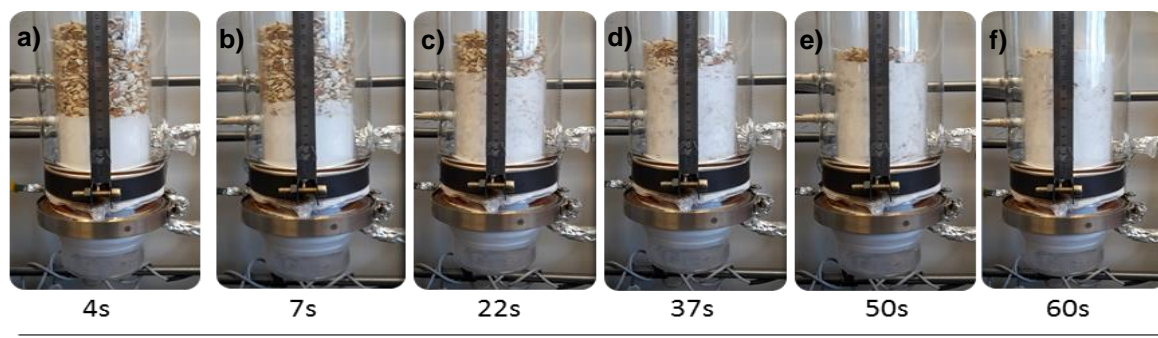


*Figure 2: Snapshots of mixing patterns of CA/OP-16 binary mixture at a flow rate of 1500 Nl/h .*

For each investigated binary mixture (i.e., FS/OP, CS/OP, FA/OP and CA/OP) several fluidization tests were performed by increasing the biomass weight fraction ($X_B$) in the bed. This allowed both to study the effect of the bed content on the characteristic velocities of the investigated systems (i.e., minimum and complete fluidization velocities) and to determine their maximum batch loading, i.e. the critical value of $X_B$ beyond which the fluidization quality deteriorates (e.g., channeling, segregation, slugging). As regards fluidization experiments involving binary mixtures, the initial arrangement of the bed was such that the bed components were completely segregated with the biomass particles on the top of the bed (see Figure 2a). To obtain such a state, the two bed components were poured into the reactor in sequence. Starting from this fixed bed configuration, first the airflow rate was quickly set at 1500 Nl/h (corresponding to a superficial gas velocity of about 5 cm/s) and then gradually increased until a slugging or turbulent regime was observed. In most of the tests performed in this work, an air flow-rate of 1500 Nl/h proved to be sufficient to ensure a gradual transition (in less than 1 minute) from the initial fully segregated fixed bed configuration (Figure 2a) to a well-mixed regime (Figure 2f) characterized by a uniform distribution of particles in the bed, as showed by the snapshots in Figure 3, which refers to CA/OP-16 binary mixture.

*Table 2: Experimental operating variables and binary mixture characteristic velocities*

| Binary mixtures | OP weight fraction, % wt. | OP volume fraction*, %vol. | H/D ratio**, - | $U_{mf}$, cm/s | $U_{cf}$, cm/s |
|---|---|---|---|---|---|
| FS/OP-0 | 0 | 0 | 2.1 | 1.99 | - |
| FS/OP-1 | 1.03 | 6.25 | 2.3 | 2.27 | 5.08 |
| FS/OP-2 | 2.04 | 12.07 | 2.3 | 2.35 | 5.62 |
| FS/OP-3 | 2.97 | 16.67 | 2.3 | 2.62 | 6.19 |
| FS/OP-4 | 4.18 | 18.92 | 2.2 | 3.17 | 6.53 |
| CS/OP-0 | 0 | 0 | 2.2 | 3.75 | - |
| CS/OP-1 | 1.04 | 5.56 | 2.3 | 4.00 | 5.24 |
| CS/OP-3 | 2.96 | 15.85 | 2.3 | 3.79 | 5.10 |
| CS/OP-5 | 4.85 | 20.93 | 2.4 | 4.23 | 5.66 |
| FA/OP-0 | 0 | 0 | 2.3 | 0.68 | - |
| FA/OP-1 | 0.99 | 2.86 | 2.3 | 0.79 | 1.21 |
| FA/OP-3 | 2.91 | 9.33 | 2.4 | 0.76 | 1.72 |
| FA/OP-5 | 4.82 | 15.00 | 2.3 | 0.79 | 1.71 |
| FA/OP-7 | 6.61 | 19.06 | 2.0 | 0.77 | 2.04 |
| FA/OP-9 | 9.17 | 23.60 | 2.4 | 0.78 | 2.69 |
| FA/OP-11 | 10.77 | 27.66 | 2.4 | 0.76 | 2.99 |
| FA/OP-12 | 12.31 | 30.89 | 2.4 | 0.77 | 3.00 |
| FA/OP-14 | 13.86 | 32.54 | 2.4 | 0.84 | 3.01 |
| FA/OP-15 | 15.31 | 35.24 | 2.4 | 0.93 | 3.31 |
| FA/OP-17 | 16.73 | 37.73 | 2.3 | 0.86 | 3.94 |
| FA/OP-18 | 18.10 | 41.38 | 2.4 | 0.95 | 4.23 |
| CA/OP-0 | 0 | 0 | 2.3 | 2.96 | - |
| CA/OP-2 | 2.01 | 7.61 | 2.3 | 3.07 | 4.53 |
| CA/OP-4 | 4.09 | 13.33 | 2.3 | 3.09 | 4.53 |
| CA/OP-6 | 6.08 | 18.42 | 2.3 | 3.10 | 4.82 |
| CA/OP-8 | 8.05 | 24.06 | 2.3 | 3.24 | 5.53 |
| CA/OP-10 | 10.15 | 27.84 | 2.3 | 3.29 | 5.38 |
| CA/OP-12 | 12.24 | 31.58 | 2.4 | 3.38 | 5.58 |
| CA/OP-14 | 14.31 | 36.36 | 2.4 | 3.49 | 5.58 |
| CA/OP-16 | 16.36 | 37.50 | 2.3 | 3.42 | 6.10 |

*Calculated on the basis of its bulk volume.
**The static bed height, H, was measured visually by using a scale attached along the height of column.

Note that if a too high initial air flow rate was set, the system exhibited an almost plug-flow behavior, which means that all particles were transported out of the bed with little back-mixing. But, in general, both the critical air flow rate and time required to reach a well-mixed regime slightly increased by increasing the biomass weight fraction in the bed for each of the investigated binary mixtures. The classical pressure drop method based on the use of fluidization curve was adopted to determine the value of both the minimum ($U_{mf}$) fluidization velocity as the point of intersection of the straight lines corresponding to the fixed-bed and fluidized bed portions of the graph (Kunii and Levenspiel, 1991) and the complete fluidization velocity ($U_{cf}$) as the minimum value of the superficial gas velocity where a pressure drop equal to the weight of the bed per unit cross-sectional area is detected in the fluidization curve (Brachi et al., 2016). In particular, $U_{mf}$ and $U_c$ were measured upon decreasing the fluidization velocity to avoid dependence on the initial bed configuration. Hence, during each experiment, starting from the above-mentioned well-mixed regime, the air flow rate was gradually decreased to zero and the pressure drop across the bed was continuously recorded.

## 3. Results and discussion

A long list of interrelated parameters affecting the mixing/segregation behaviour of binary fluidized bed, including the size ratio, density ratio and the mass ratio of the bed components as well as the superficial gas velocity, makes its characterization particularly complex. In the present work, during each fluidization experiment, the mixing and segregation behaviour of the investigated binary systems was carefully observed, finally suggesting that bed components' density difference prevails over the size difference. In particular, tests performed on binary systems having the similar size ratio but different density (i.e., FS/OP and FA/OP; CS/OP and CA/OP) or with the similar density but different size (i.e., FA/OP and CA/OP; FS/OP and CS/OP) showed that: 1. the lower was the density difference between the bed components (FA/OP and CA/OP; CS/OP and

CA/OP), the higher was the OP weight fraction at which a critical value of the gas velocity still exists to ensure a uniform distribution of particles in the bed (well-mixed regime); 2. binary mixtures having almost the same density ratio but different size ratio (FA/OP and CA/OP; CS/OP and CA/OP) exhibited almost the same maximum biomass batch loading, i.e., 4-5 %wt. for FA/OP and CA/OP binary mixture and 16-18 %wt. for CS/OP and CA/OP (see Table 1). In more details, in this work, the maximum biomass batch loading for the investigated binary mixtures was assumed equal to the $X_B$ value beyond which starting from a fully segregate fixed bed configuration the further increase of the air flow rate above 1500 Nl/h (cf. Section 3.1) did not result in a well-mixed regime but rather in: 1. a partially segregated bed with residual biomass particles floating at the bed surface (flotsam) and exhibiting slugging regime, as shown in Figure 3a-c for the FS/OP-6 ($X_B = 6.1$ %wt.; 26.8 %vol.), CS/OP-7 ($X_B = 7.1$ %wt.; 24.6%vol.) and CA/OP-18 ($X_B = 18.4$ %wt.; 43.6 %vol.) binary mixture; 2. a partially segregated bed with biomass particles sinking to the bottom of the bed (jetsam) as shown in Figure 3d for the FA/OP-21 ($X_B = 20.7$%wt.; 45.3 %vol.) binary mixture. It is nothworthy that only in the case of Geldart A type inert bed component (i.e., γ-alumina powder), the less dense biomass particles acted as jetsam, according to the nomenclature proposed by Rowe et al. (1972), while denser inert particles revert to floatsam, upon fluidization. This outcome is in total agreement with the observations of Chiba et al. (1980), who studied the characteristics of fluidized binary mixtures in which the denser component acts as floatsam.
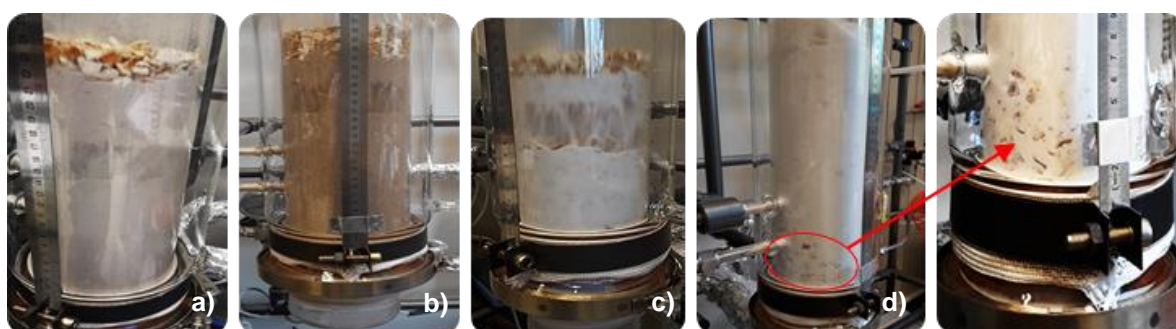


Figure 3 Segregation and slug phenomena in: a. FS/OP-6 ($X_B = 6.1$ %wt.; 26.8 %vol.); b. CS/OP-7 ($X_B = 7.1$ %wt.; 24.6%vol.); c. CA/OP-18 ($X_B = 18.4$ %wt.; 43.6 %vol.); and d. FA/OP-21 ($X_B = 20.7$%wt.; 45.3 %vol.) binary mixtures (not reported in Table 2) at high fluidization number ($U_g/U_{mf}$).

Figure 4a-c shows the fluidization curves of: a. FA/OP-5 binary mixture; b. FA/OP-17 binary system, which exhibited some undesired fluidization-related phenomena including in-bed channeling, bed cracks, small and/or big lump formation (i.e., localized accumulation of biomass particles) during bed defluidization; and c. FA/OP-23 binary mixture ($X_B = 23.1$ %wt.; 48.6 %vol.; not reported in Table 2), which exhibited bed segregation and slugging phenomena upon bed defluidization. The obtained trends suggest that, when the biomass weight fraction in the bed was controlled in order to avoid undesired bed segregation or slugging phenomena, which is the case of test conditions listed in Table 2, the defluidization curve of polydisperse binary mixtures presents the same pressure drop profile as binary mixtures consisting of regular spherical particles differing only in one of their constitutive properties (Formisani et al., 2008), thus making the graphical determination of $U_{mf}$ and $U_{cf}$ appropriate (Figure 4).
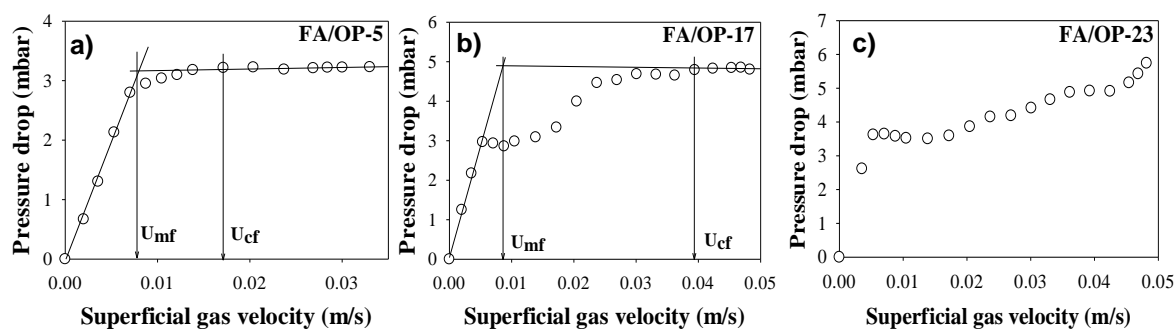


Figure 4 Pressure drop as a function of superficial gas velocity for binary mixtures: a. FA/OP-5; b. FA/OP-17; and c. FA/OP-23.

Table 2 reports the values of the velocities of minimum and complete fluidization obtained for the investigated binary mixtures. The same data were represented on graphs in Figure 5 as a function of the OPs weight fraction ($X_B$) in the bed. Data show that all the characteristic velocities increased with the increase of the biomass weight fraction in the bed, with a more marked effect in the case of FS/OP binary system (see the largest slopes in Figure 5b). It also results that the complete fluidization velocity ($U_c$) always increased faster than the minimum fluidization velocity ($U_f$) for each binary system when the OPs weight fraction was incremented; this was particularly evident for mixtures involving low density solids (i.e., FA/OP and CA/OP).
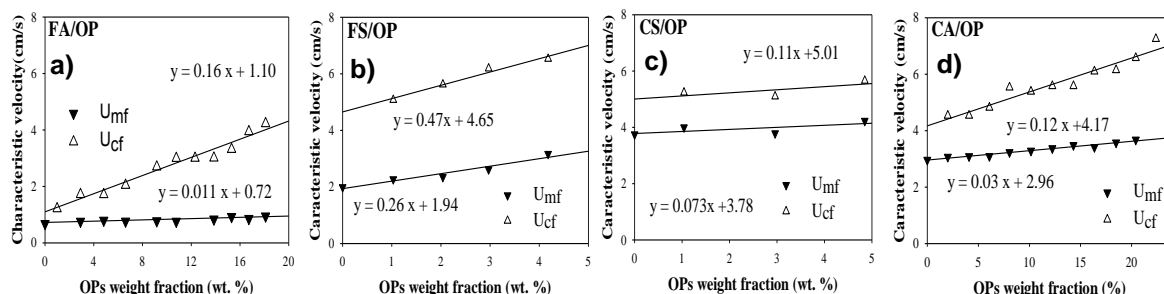


*Figure 5 Minimum and complete fluidization velocities as a function of biomass weight fraction in the bed: for binary systems : a. FA/OP; b. FS/OP; c. CA/OP; and d. CS/OP.*

## 4. Conclusion

The present work studied the fluidization and segregation behaviour of poly-disperse binary mixtures of biomass and inert particles. In particular, air-dried orange peels slabs (0.5 cm x 0.5 cm) were used as biomass feedstock while several granular solids with the same density but different size or with the same size but different density were tested as inert bed component in order to determine the prevalence of the effect of either size or density on the fluidization and segregation behavior of the investigated binary systems. Tests at different $X_B$ in the bed were also performed for each of the investigated binary systems. The notable findings of this study were that: 1. the bed components' density difference prevails over the size difference in determining the mixing/segregation behavior of binary fluidized bed; 2. if the dense particles are sufficiently small (Geldart A type) and in sufficiently low concentration (< 60 % by volume) to be incorporated in the interstices of a packed bed of the larger ones, then the coarse and less dense pieces of biomass (Geldart D type), upon fluidization, behave as jetsam; 3. conversely, if the dense particles are sufficiently large in size (Geldart B type) and in sufficiently low concentration the less dense biomass particles (Geldart D type) behave in the conventional way, i.e. revert to flotsam;4. the velocities of minimum and complete fluidization increase with the increase of the biomass weight fraction in the bed.

## References

Brachi P., Miccio F., Miccio M., Ruoppolo G, 2016; Torrefaction of Tomato Peel Residues in a Fluidized Bed of Inert Particles and a Fixed-Bed Reactor, Energy Fuels 30, 4858-4868.
Bruni G., Solimene R., Marzocchella A., Salatino P., Yates J.G., Lettieri P., Fiorentino M., 2002, Self-segregation of high-volatile fuel particles during devolatilization in a fluidized bed reactor, Powder. Technol. 128, 11-21.
Chiba S., Nienow A.W., Chiba T., Kobayashi H., 1980, Fluidised binary mixtures in which the denser component may be flotsam, Powder. Technol. 26, 1–10.
Cui H., Grace J.R, 2007, Fluidization of biomass particles: A review of experimental multiphase flow aspects, Chem. Eng. Sci. 62, 45-55.
Formisani B., Girimonte R., Longo T., 2008, The fluidization process of binary mixtures of solids: Development of the approach based on the fluidization velocity interval, Powder. Technol. 185, 97-108.
Kunii D., Levenspiel O., 1991, Fluidization Engineering, 2nd ed., MA, USA: Butterworth-Heinimann Newton; 1991
Rowe P.N., Nienow A.W., Agbim A.J., 1972, The mechanisms by which particles segregate in gas fluidized beds-binary systems of near-spherical particles, Trans. Inst. Chem. Eng. 50, 310-320.
Ruoppolo G., Miccio F., Brachi P., Picarelli A., Chirone R., 2013, Fluidized bed gasification of biomass and biomass/coal pellets in oxygen and steam atmosphere , Chemical Engineering Transactions 32, 595-600.
Volpe M., Panno D., Volpe R., Messineo A., 2015, Upgrade of citrus waste as a biofuel via slow pyrolysis, J. Anal. Appl. Pyrol.115, 66-76.